

# Modeling and Simulations of Adhesion between Carbon Nanotubes and Surfaces

N. R. Paudel<sup>1</sup>, A. Buldum<sup>1,2</sup>, T. Ohashi<sup>3</sup> and L. Dai<sup>4</sup>

<sup>1</sup>Department of Physics, The University of Akron

<sup>2</sup>Department of Chemistry, The University of Akron,

<sup>3</sup>Honda Research Institute USA Inc.

<sup>4</sup>Department of Chemical and Materials Engineering, University of Dayton

## ABSTRACT

Recent experiments showed that there are very strong adhesion forces between nanotubes and surfaces. These forces were much stronger than the adhesion forces of Gecko's foot hairs on substrates. Thus, nanotubes become candidates to be used in dry adhesives. Here, we present theoretical investigations on the adhesion between nanotubes and graphite surfaces. Molecular dynamics simulations and energy minimization calculations were performed. Layer by layer deformations of the nanotube tips were observed. Parallel and perpendicular components of the forces were calculated for different contact angles of nanotubes. The adhesion forces are found to be maximized at 15° angles with respect to surface normal.

**Keywords:** Nanotubes, Adhesion, Gecko's Foot, Molecular Dynamics

## 1 INTRODUCTION

Carbon nanotubes (CNTs) have attracted great interest in the field of nanotechnology because of their remarkable mechanical, electrical and transport properties [1-5]. The mechanical properties of nanotubes are very important as many potential applications depend on these properties. Over the past couple of years, there have been many studies on mechanical properties and deformation on CNTs such as bending, buckling, twisting and curvature effects using molecular dynamics (MD) simulations [4]. With the development of new experimental techniques, the buckling behavior of the CNTs has been observed under large deformation [6].

Recent experiments showed that there are very strong adhesion forces between nanotubes and surfaces. Yurdumakan et. al. [7] measured the adhesion force on multiwalled carbon nanotubes. In the experiment, they formed MWNT brushes on PMMA polymer surfaces. Then, scanning probe microscopy was used to measure the strong adhesion forces of the MWNT brushes. They found that the forces were 200 times higher than that of gecko's foot hairs[8]. Thus, nanotubes are good candidates to be used in dry adhesives.

In this research study, we perform theoretical investigations of CNTs interacting with surfaces. To study the deformation behavior and adhesion of CNTs, atomistic simulations of capped armchair (10,10) nanotubes with two different lengths are performed on rigid and relaxed graphite surfaces. There had been many theoretical studies of CNT tips interacting with surfaces[9-13]. These studies were mainly focused on employing CNTs as SPM tips. We started with a similar system, however, beside studying the deformation of CNTs, we also focused on parallel and perpendicular components of the forces for different contact angles to investigate the adhesive behavior of nanotubes.

## 2 MODEL

Atomic models of (10, 10) armchair single-wall nanotubes were created and combined with atomic models of graphite surfaces which are multilayer periodic graphite lattice structures. Two capped nanotubes of different lengths were selected such that the shorter tube had 790 atoms and the longer tube had 1990 atoms. The lengths between two extreme ends of the tubes were 46.5 Å and 122 Å, respectively. These tubes were then combined with graphite surfaces consisting 10 layers. In the longer tube case, the lattice constants of the overall structure were  $a = 49.2$  Å,  $b = 49.2$  Å and  $c = 163$  Å where,  $a = 36.9$  Å,  $b = 36.9$  Å and  $c = 86$  Å were chosen for the shorter tube case. 120 atoms of the nanotube from the uncapped end were chosen to be fixed. The nanotubes were initially positioned at 6 Å above the top layer of the graphite surface. The simulations were performed by using Cerius<sup>2</sup> with the Universal Force Field [10].

During the simulations, the fixed nanotube atoms were moved towards the surface in the increments of 0.1 Å for energy minimization calculations and 0.2 Å for the molecular dynamics simulations. In MD simulations, the entire system was allowed to equilibrate for 5000 steps initially and then moved towards the surface. There were 500 MD steps in between each increment of the displacement of the tip. All MD simulations were performed at constant NVT. The temperature was selected as 10 K and the time step was 0.001 PS.

### 3 DEFORMATION OF THE NANOTUBES AND ADHESION FORCES

The first series of simulations were energy minimization calculations and nanotubes were facing hollow, top1 and top2 atomic sites of graphite surface. These atomic sites are shown in figure 1.

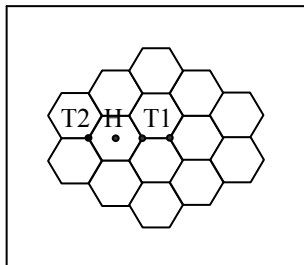


Figure 1: The hollow (H), top1 (T1) and top2 (T2) sites on the top-most layer of the graphite surface.

Energy minimization calculations were performed for both short and long nanotubes on rigid and relaxed surfaces. The total potential energy ( $E$ ) was calculated during the simulations and the variation of  $E$  as a function of  $z$  displacement for a short nanotube on three different atomic sites is presented in figure 2. In the figure, the first major peak represents the critical position of the tip in which the repulsive interaction between the graphite surface and tip reaches a maximum. When the tip was moved closer to the surface, a layer of carbon atoms from the tip moved into the tube which resulted with the first deformation of the tip and caused the energy to drop. Snapshots of the tip deformation for the hollow atomic site case are shown in figure 3.

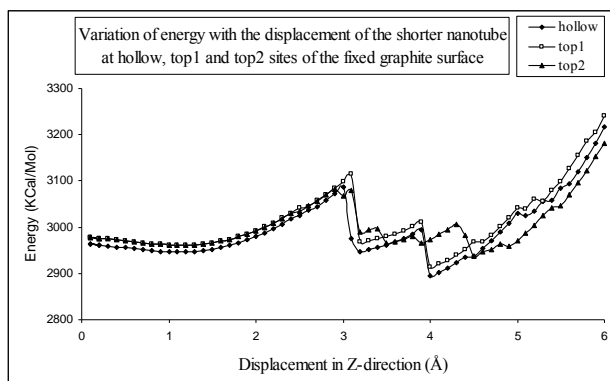


Figure 2: Variation of the total potential energy as a function of tip displacement for the shorter nanotube on a fixed graphite surface. The nanotube tip was initially 6Å above the surface. Positive  $z$ -direction is towards the surface.

When the tip moves toward the graphite surface, the nearest atoms of the capped end are first attracted by the graphite layers up to a critical position then repulsive forces push them back along the tube axis. When the tip moves further, the repulsive forces are increased that causes layer by layer the compression of the cap into the interior of the nanotube. The sharp end of the cap changes gradually from an original concave shape to a convex shape which also was observed in previous simulations [11]. The symmetrical deformation of the inversed cap of the tip was observed for the hollow site but not necessarily for the top1 and the top2 sites. Two results from these calculations appeared to be interesting at this point. One is the layer by layer compression of the tip surface which is related with the discrete nature of the tip deformation. Another is the atomic surface site dependence of the energy variation and deformation. How atoms are positioned with respect to each other is important for the energy variation and deformation of the nanotube cap.

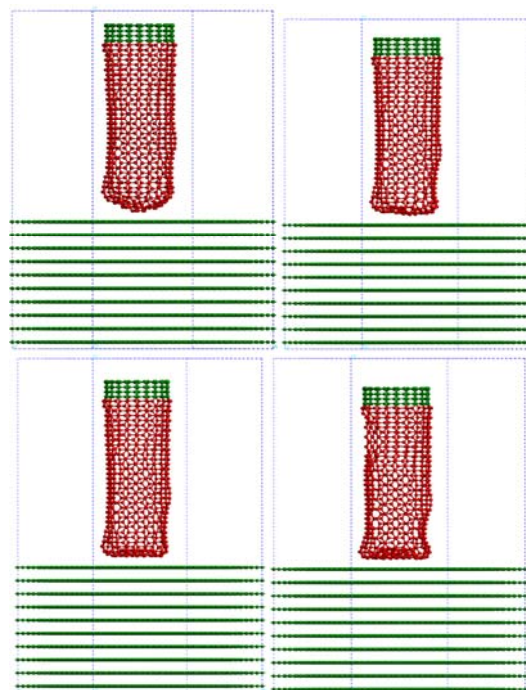


Figure 3: Snapshots from the energy minimization of the interaction of a capped [10, 10] nanotube with fixed graphite layers at hollow position for (a)  $\Delta Z = 2 \text{ \AA}$  (b)  $\Delta Z = 3.5 \text{ \AA}$  (c)  $\Delta Z = 4.3 \text{ \AA}$  and (d)  $\Delta Z = 6 \text{ \AA}$ .

After further compression, the structural deformation of the side wall increases gradually and then changes into buckling of the nanotube. The large deformation of the longer nanotube with buckling, bending and slipping from MD simulations is presented in figure 4. As it can be seen in the figure, the front part of the nanotube after the onset of buckling makes an angle with the graphite surface. After

buckling and bending, the slipping of the tip on the graphite surface was observed.

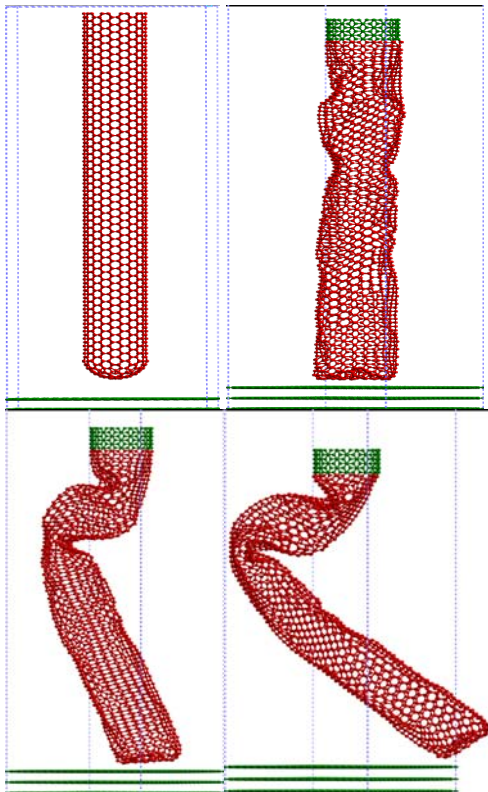


Figure 4: Snapshots from the molecular dynamics simulations of a long capped (10, 10) nanotube on a fixed graphite surface at hollow position for (a)  $\Delta Z = 0 \text{ \AA}$  (b)  $\Delta Z = 10 \text{ \AA}$  (c)  $\Delta Z = 20 \text{ \AA}$  and (d)  $\Delta Z = 40 \text{ \AA}$ .

Another series of simulations were performed for different contact angles of nanotubes on graphite surfaces. The contact angle (or impact angle) here is the angle between the nanotube axis and the normal of the graphite surface as shown in the figure 5.

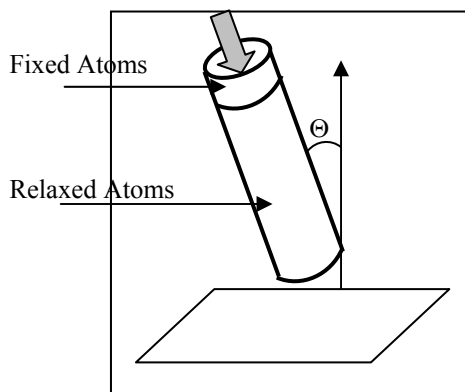


Figure 5: Schematic diagram of the tilted nanotube. The contact or impact angle  $\Theta$  is defined with respect to the surface normal.

Simulations were performed for seven impact angles in intervals of  $5^\circ$  from 0 to 30 degrees. The nanotubes were initially positioned  $6 \text{ \AA}$  above the graphite surface and moved along the axes of the nanotubes (the direction of the motion is shown by an arrow in figure 5) up to  $20 \text{ \AA}$  axial displacement. One important quantity for the adhesion is the length of front part of the nanotube after buckling (i.e. buckling length). The front part would become parallel to the surface after further compression and the main contribution to the adhesion force would be coming from this part. The buckling length of a buckled nanotube is from the point of buckling to the capped end of the nanotube. The buckling length as a function of impact angles is presented in figure 6.

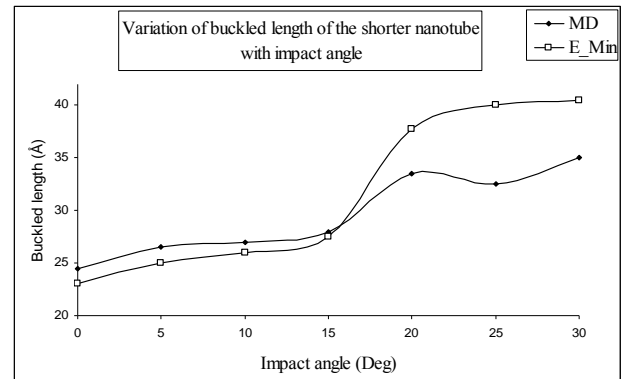


Figure 6: Impact angle dependence of the buckling length of the shorter tube determined from MD simulations and energy minimization calculations.

In the figure, we can see the variation of buckling length of the shorter tube, which increases slowly at first with the impact angle, and then increases rapidly between 15 and 20 degrees and finally becomes nearly constant after 25 degree. Beyond 30 degree slipping occurs quickly so that buckling of the nanotube could be observed rarely beyond this point. One can clearly see in the figure that the buckling length change appears to be significantly larger in the energy minimization case. This is due to the temperature dependent relaxation of the atoms in the MD simulations. Similar results were also obtained for the longer nanotube.

By performing MD simulations, the maximum force on the nanotubes for different impact angles were determined. Maximum force values for different impact angles are presented in figure 7. The results show that the maximum force depends on the impact angle and has a maximum at 15 degrees. This angle coincides with the angles where sudden change in the buckling length was occurred. The components of the adhesion forces were investigated also. The parallel components of forces were much weaker than the perpendicular components. On the other hand, for tilted orientations of the nanotubes, the

parallel component increases with the increase of the impact angle.

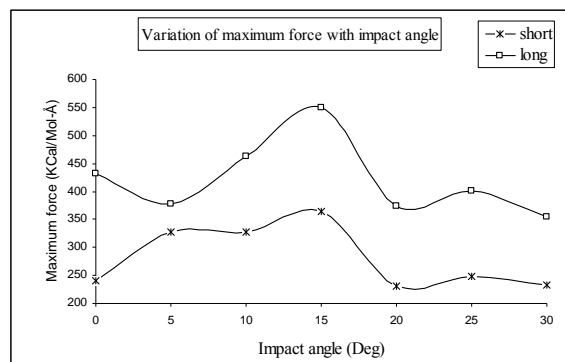


Figure 7: Impact angle dependence of the maximum force experienced by the atoms of tip surface.

## 4 CONCLUSIONS

Theoretical investigations on the adhesion between nanotubes and graphite surfaces were performed. Atomistic simulations of capped armchair (10,10) nanotubes with two different lengths on rigid and relaxed graphite surfaces were carried out. The layer by layer compression of the tip surface was observed which is related with the discrete nature of the tip deformation. The total potential energy and deformation of the nanotube cap were dependent on the local atomic surface sites. The buckling length increased slowly at first with the impact angle, and then increased rapidly between 15 and 20 degrees. The maximum force on the nanotube depends on the impact angle and has a maximum at 15 degree.

## REFERENCES

- [1] S. Iijima, Nature, 354 56, 1991.
- [2] J. P. Lu, Phys. Rev. Lett., 79, 1297, 1997
- [3] B. I. Yakobson, C. J. Brabec, and J. Bernholc, Phys. Rev. Lett., 76, 2511, 1996.
- [4] J. Mintmire, B. Dunlap and C. White, Phys. Rev. Lett., 68, 631, 1992.
- [5] A. Buldum and J. P. Lu, Phys. Rev. Lett., 91, 236801, 2003.
- [6] G. Cao and X. Chen, Phys. Rev. B, 74, 165422, 2006
- [7] B. Yurdumakan, N. R. Raravikar, P. M. Ajayan and A. Dhinojwala, Chem. Communication, 3799, 2005
- [8] K. Autumn, Y. A. Liang, S. T. Hsieh, W. Zesch, W. P. Chan, T. W. Kenny, R. Fearing and R. J. Full, Nature, 405, 681, 2000.
- [9] N. Yao and V. Lordi, Phys. Rev. B, 58, 12649, 1998.
- [10] A. K Rappe, C. J. Caswit, K. S. Colwell, W. A. Goddard III and W. M. Skiff, J. Am. Chem. Soc., 114, 10024, 1992.

[11] S. P. Ju, C. L. Weng and C. H. Lin, J. Appl. Phys., 95, 5703, 2004

[12] J. A. Harrison, S. J. Stuart, D. H. Robertson and C. T. White, J. Phys. Chem. B, 101, 9682, 1997.

[13] A. Grag and S. B. Sinnott, Phys. Rev. B, 60, 13786, 1999